

Optical interferometry of High-Mass X-ray Binaries: Resolving wind, disk and jet outflows at sub-milliarcsecond scale

Idel Waisberg¹, Jason Dexter¹, P.-O. Petrucci², Guillaume Dubus²,
Karine Perraut² and GRAVITY Collaboration[†]

¹Max Planck Institute for extraterrestrial Physics,
Giessenbachstr., 85748 Garching, Germany
email: idelw@mpe.mpg.de

²Univ. Grenoble Alpes, CNRS, IPAG
Box 515, F-38000 Grenoble, France

Abstract. Because of their small angular size < 1 mas, spatial information on High-mass X-ray binaries (HMXB) has typically been inferred from photometry or spectroscopy. Optical interferometry offers the possibility to spatially resolve such systems, but has been traditionally limited to bright targets or low spectral resolution. The VLTI instrument GRAVITY, working in the near-infrared K band, achieves unprecedented precision in differential interferometric quantities at high spectral resolution, allowing to study HMXBs through the lens of optical interferometry for the first time. We present GRAVITY observations on two X-ray binaries: the microquasar SS 433 and the supergiant HMXB BP Cru. The former is the only known steady super-Eddington accretor in the Galaxy and is in a unique stage of binary evolution, with probable ties to at least part of the ULX population. With GRAVITY, we resolve its massive winds and optical baryonic jets for the first time, finding evidence for powerful equatorial outflows and photoionization as the main heating process along the jets. BP Cru harbors an X-ray pulsar accreting from the wind of its early-blue hypergiant companion Wray 977. The GRAVITY observations resolve the inner parts of the stellar wind and allow probing the influence of the orbiting pulsar on the circumstellar environment.

Keywords. techniques: interferometric — stars: binaries: close — stars: circumstellar matter — stars: winds, outflows — infrared: stars — X-rays: binaries — stars: individual: BP Cru — stars: individual: SS 433

1. Introduction

Direct spatial information on X-ray binaries has traditionally been limited to radio wavelengths, with Very Long Baseline Interferometry enabling \sim mas spatial resolution. The movement of individual radio jet blobs, for example, has been imaged in many microquasars (e.g. Vermeulen *et al.* 1993, Mirabel & Rodriguez 1994). Optical interferometry, on the other hand, can achieve the necessary sub-mas resolution to spatially resolve such systems at scales comparable to the binary orbit $a_{orb} \lesssim 1$ mas, but has been limited to bright targets or low spectral resolution. This has changed with the GRAVITY instrument at the Very Large Telescope Interferometer (VLTI), which has achieved unprecedented precision in differential interferometric observables at high

[†] GRAVITY is developed in a collaboration by the Max Planck Institute for Extraterrestrial Physics, LESIA of Paris Observatory and IPAG of Universit Grenoble Alpes / CNRS, the Max Planck Institute for Astronomy, the University of Cologne, the Centro Multidisciplinar de Astrofísica Lisbon and Porto, and the European Southern Observatory.

spectral resolution in the near-infrared K band (GRAVITY Collaboration *et al.* 2017a). Even though the canonical imaging resolution of GRAVITY is $\approx \frac{\lambda}{B} \approx 3$ mas for baseline lengths ~ 100 m, spectral differential interferometry allows resolving sub-mas structures through differential visibilities across strong emission lines.

Here we present GRAVITY observations of two X-ray binaries: the canonical wind-accreting BP Cru / GX 301-2, where we resolve the deep layers of the donor star wind to probe the effects of the gravitational and radiation fields of the pulsar companion, and the microquasar SS 433, where we resolve the super-Eddington outflows in the form of baryonic jets, wind and equatorial outflows.

2. Resolving the Stellar Wind in BP Cru / GX 301-2

BP Cru / GX 301-2 is one the canonical wind-accreting High-Mass X-ray Binaries, consisting of a slowly rotating X-ray pulsar accreting from the wind of its hypergiant (B1Ia+; Kaper, van der Meer & Najarro 2006) donor star, called Wray 977. The latter is very massive ($\gtrsim 40M_{\odot}$) and luminous ($5 \times 10^5 L_{\odot}$), with a very high mass-loss rate $\sim 10^{-5} M_{\odot}/\text{year}$, leading to particularly strong emission lines formed in an extended wind. It is relatively nearby (3 kpc), making it an ideal target for high spectral resolution optical interferometry, capable of resolving the inner parts of its wind, through which the pulsar moves in its unusually eccentric ($e = 0.46$) orbit. The gravitational field of the pulsar is expected to lead to the formation of a wind stream with enhanced density, and in fact the very modulated X-ray light curve has been shown to be consistent with the presence of an accretion stream, which the pulsar crosses twice per orbit (Leahy & Kostka 2008). The X-ray flux from the pulsar is also expected to affect the wind of Wray 977, leading to further distortions in its structure (e.g. Blondin 1994, Cechura & Hadrava 2015).

The K band spectrum of BP Cru contains two strong emission lines of Br γ and He I 2.06 μm . The GRAVITY observations of this system (Waisberg *et al.* 2017; Figure 1) show differential visibility amplitudes and phases across the emission lines, allowing to probe the spatial structure of the inner portions of the wind. They imply a very extended wind (FWHM $\sim 3 - 7R_{*}$) that is also asymmetric across the line (being more extended on the blue/approaching part), as well as differential visibility phases that imply an asymmetry relative to the continuum and which are also stronger on the approaching part of the line. One possibility is that such asymmetries are caused by X-ray ionization of the stellar wind or by the putative accretion stream in this system. We can also compare the interferometric data with predictions from stellar wind codes. Figure 2 shows the intensity profiles of the near-infrared continuum and emission lines as a function of impact parameter as calculated with the stellar wind atmosphere code CMFGEN (Hillier & Miller 1998) with parameters derived from optical spectroscopy of BP Cru (Kaper, van der Meer & Najarro 2006). They can be directly compared to the interferometric data (black lines in Figure 1). The overall agreement on the spatial extent of the Br γ line is good, but spherically-symmetric models naturally cannot explain the asymmetries detected (e.g. they produce zero differential visibility phases).

Further observations are needed to disentangle natural variability from a wind from distortions caused by the gravitational and radiation fields of the pulsar. In particular, because the pulsar is on an eccentric orbit ($P_{orb} = 41.5$ days), comparing the spatial structure of the wind between apastron and periastron should be particularly promising. Another viable approach is to compare the spatial structure of the wind in BP Cru to isolated blue hypergiants of similar spectral type. This will help to constrain and characterize the influence of the pulsar on its environment, which is important for understanding the complex wind accretion process in HMXBs.

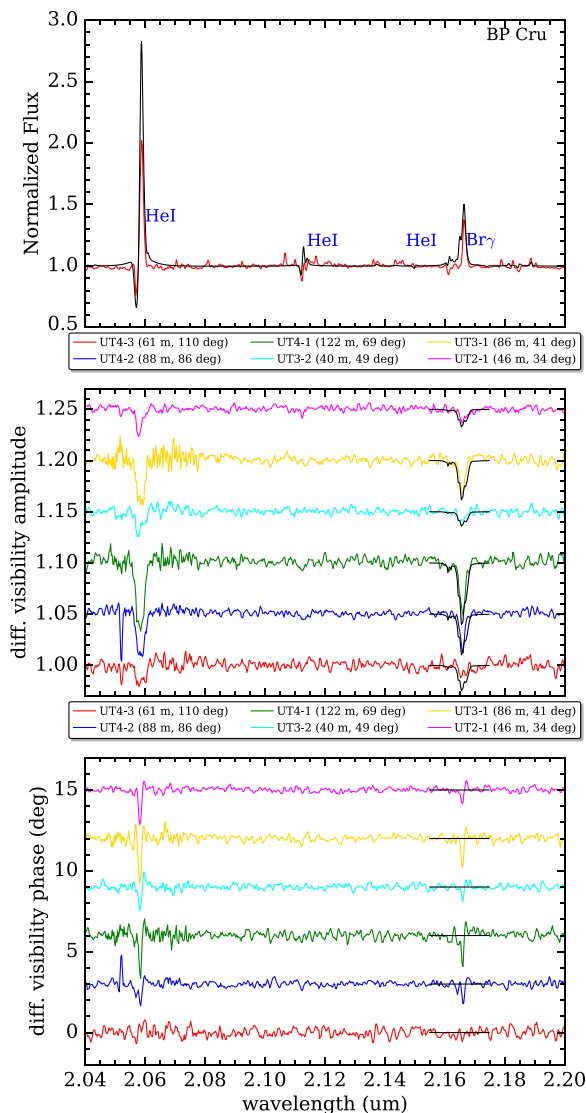


Figure 1. K band spectrum and differential visibility amplitude and phases in the GRAVITY observations of BP Cru. A CMFGEN stellar atmosphere model with parameters derived from optical spectroscopy is shown in black (visibilities are only computed for Br γ where the strength of the line is better matched). The strength of the differential visibility amplitudes are in good agreement with the model but spherically symmetric models cannot explain the nonzero differential visibility phases across the line.

3. Resolving the Super-Eddington Outflows in SS 433

SS 433 was the first microquasar discovered through the broad emission lines of hydrogen and helium moving across its optical spectrum spanning large redshifts (Margon *et al.* 1979), which arise from precessing, relativistic (0.26c) baryonic jets (Fabian & Rees 1979). The supercritical accretion disk in SS 433 outshines its donor star at all wavelengths and drives powerful outflows, not only in the form of jets but also in strong and broad “stationary” (as opposed to the jets) emission lines (Fabrika 2004). The estimated mass-loss rate $\dot{M} \sim 10^{-4} M_{\odot}/\text{yr}$ (Fuchs, Miramond & Ábrahám 2006) clearly

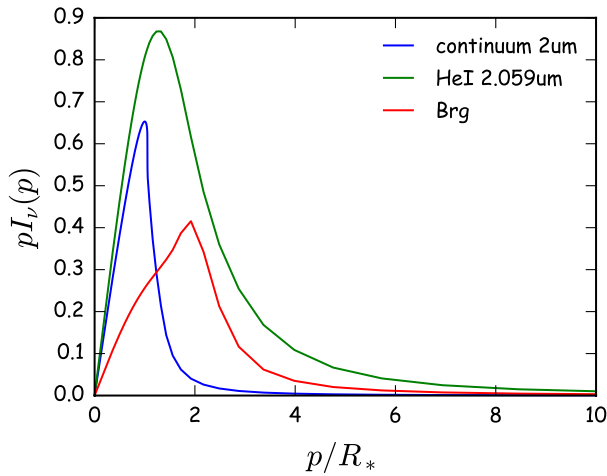


Figure 2. Intensity profile of the near-infrared continuum and K band emission lines as a function of impact parameter (p), as calculated with a CMFGEN stellar wind model for Wray 977. A 2d Fourier Transform of the profiles can be directly compared to the optical interferometry data as shown in Figure 1.

establishes SS 433 as an outflow-regulated supercritically accreting system. With a binary orbit size $a_{orb} = \left(\frac{M}{40M_{\odot}}\right)^{1/3} \times 0.07$ mas (where M is the total binary mass) resolving the inner parts of the outflow is not possible with current single telescopes, but is within the grasp of high precision spectro-differential optical interferometry.

The first GRAVITY observations of SS 433 happened in July 2016 and the results were presented in [GRAVITY Collaboration *et al.* 2017b](#) (Paper I). The optical jets were resolved for the first time, and their emission profile was shown to follow an exponential distribution which peaks at the center of the binary and decays on a scale ≈ 2 mas, in contradiction with previous indirect estimates from spectroscopic monitoring of the moving $H\alpha$ lines which suggested that the optical bullets had a typical emission peak ≈ 5 mas and extend up to $\gtrsim 10$ mas from the central binary ([Borisov & Fabrika 1987](#)). The observations also spatially resolved the $Br\gamma$ stationary line, revealing an extended structure dominated by emission following the jet direction (suggestive of bipolar outflow). Here we present preliminary results on the second set of GRAVITY observations of SS 433. These consist of three observations taken over a period of four nights (2017-07-07, 2017-07-09 and 2017-07-10).

3.1. The Equatorial Outflows

Figure 3 shows the model-independent centroid displacements across the $Br\gamma$ stationary line derived from the differential visibility phases in one of the 2017 observations. The line is clearly dominated by an equatorial structure perpendicular to the jets. The presence of Gaussian components from a rotating circumbinary ring in stationary emission lines such as $H\alpha$ and $Br\gamma$ has been inferred from previous spectroscopic observations (e.g. [Blundell, Bowler & Schmidtobreick 2008](#), [Perez & Blundell 2009](#), [Bowler 2010](#)), where the assumption of Keplerian rotation at the innermost stable circumbinary radius has been used to derive a total binary enclosed mass $\gtrsim 40M_{\odot}$ suggestive of a massive black hole as the compact object.

Figure 4 shows the spectrum centered on the $Br\gamma$ line, as well as the differential visibility amplitudes and phases across two representative baselines. For baselines aligned with the equatorial direction, the “S-shape” signature typical of rotation is very clear, in contrast with baselines more aligned with the jet direction. The decay in visibility

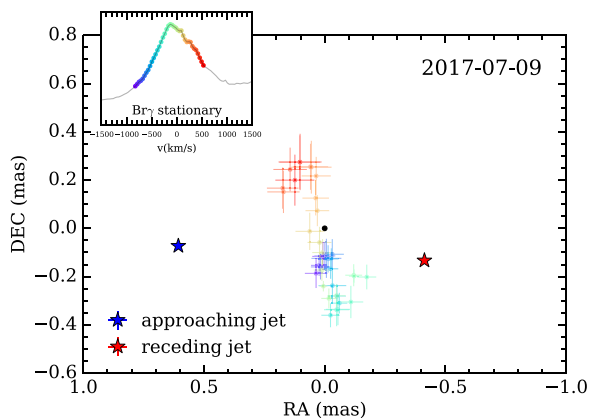


Figure 3. Model-independent centroid shifts across the Br γ stationary line in SS 433. The centroids for the jet emission lines are also shown. The stationary emission has a clear equatorial direction in 2017. The insets show the Br γ line spectrum. An angular size of 1 mas corresponds to 5.5 AU for the assumed distance 5.5 kpc.

amplitude (indicating structure more extended than the continuum, which is partially resolved) requires the presence of a second extended component which we interpret as a spherical wind. This component is also responsible for the high-velocity $\gtrsim 1000$ km/s wings of the emission line, and with a FWHM ~ 6 mas it engulfs the entire binary system and must therefore be optically thin.

We fit the data with a Keplerian disk model, which results in a too high enclosed mass $\gtrsim 400M_{\odot}$, following from a deprojected rotational velocity ≈ 260 km/s at an outer disk radius ≈ 1.0 mas. This would suggest an intermediate mass black hole as the compact object, which would be in severe tension with all the known properties of the object (Fabrika 2004.) Furthermore, the resulting inner radius in the model is $\lesssim 0.1$ mas, which would be smaller than the semi-major axis for such a high mass and the disk would therefore not be circumbinary. We rather interpret the disk as an equatorial rotating outflow (which is also the model shown in Figure 4), with a resulting outflow radial velocity ~ 240 km/s. Equatorial outflows in SS 433 are typically seen in radio images either as outflowing knots (e.g. Paragi *et al.* 1999) or as a smooth structure, which has been called the “radio ruff” (Blundell *et al.* 2001). We postulate that the equatorial structure we interpret traces the inner portions of these outflows, which are clearly rotating. We note that in Paper I the equatorial structure was not detected; rather, the stationary Br γ line emission is dominantly along the jet direction, suggestive of a bipolar outflow. This suggests that the equatorial structure in SS 433 is unstable.

An interesting aspect of the equatorial outflows is that they carry a very large amount of specific angular momentum. The rotational velocity is ~ 220 km/s for an outer radius ~ 0.7 mas, which corresponds to a specific angular momentum $\gtrsim 10\times$ the specific orbital angular momentum of the compact object, assuming a radial velocity semi-amplitude ~ 200 km/s (Fabrika & Bychkova 1990) and a total binary mass $\lesssim 40M_{\odot}$. The orbital angular momentum of the donor star is even lower since the mass ratio $q < 1$ (Cherepashchuk, Postnov & Belinski 2018). We propose that the equatorial outflows may be driven by the supercritical accretion disk and carry angular momentum either from the inner portions of the disk (Blandford & Payne 1982) or from the compact object itself through a magnetic propeller effect (Illiarionov & Sunyaev 1975). We note that our first spatially resolved observations of a stationary line in SS 433 cast severe doubt on previous mass estimates that assumed that their typical double-peaked structure arises in an accretion disk (Fillipenko *et al.* 1988; Robinson *et al.* 2017) or in a circumbinary ring in Keplerian rotation (Blundell, Bowler & Schmidtbreick 2008; Bowler 2010),

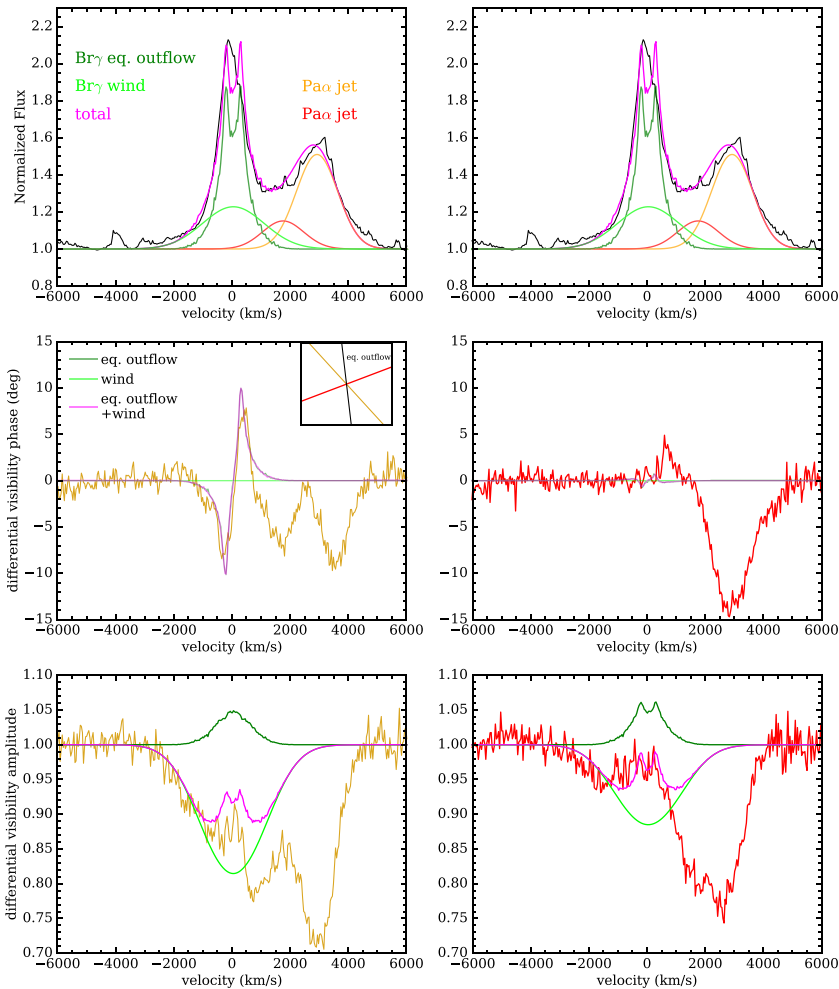


Figure 4. The **top** row shows the spectrum centered on the Br γ stationary line. The latter is decomposed into an equatorial outflow and a spherical wind. The former is responsible for the S-shape signatures in the differential visibility phases (**middle** row) for baselines which are close to perpendicular to the jet (left), and show almost no signature on baselines more aligned with the jet (right). The inset shows the position angle of the outflow from the fit as well as the baseline directions on the sky plane. The **bottom** row shows the differential visibility amplitudes. The equatorial outflow alone would lead to an increase in visibility amplitude across the Br γ line. The extended wind component can explain both the high velocity wings $\gtrsim 1000$ km/s in the spectrum as well as the net decrease in visibility amplitude across the line. Note that there are two Pa α emission lines from the receding jet which are blended with the Br γ stationary line on its red side, and which also create strong visibility signatures. The model fits were done for all the components simultaneously, but here we show only the visibility model for the stationary line for clarity.

which concluded that the compact object must be a neutron star or massive black hole, respectively. We consider that the nature of the compact object is still unknown.

3.2. The Optical Jets

In the 2017 observations, the precessional phase of the jets was ≈ 0.9 (where phase 0.0 corresponds to lowest inclination/maximum visibility of the accretion disk). The strongest

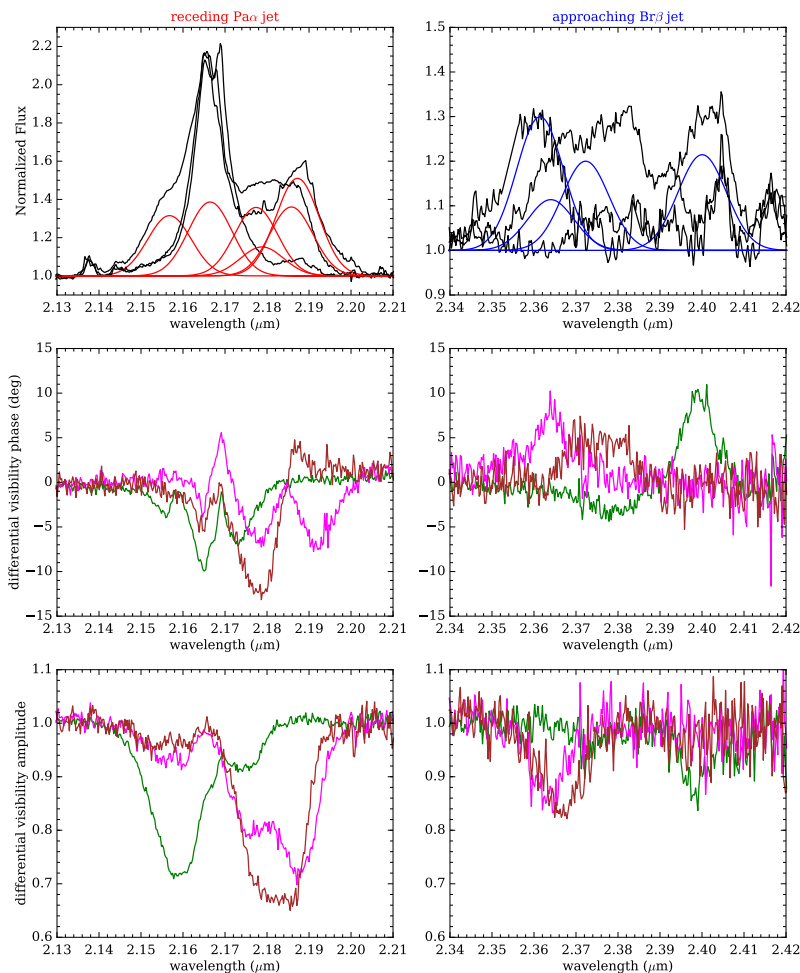


Figure 5. Same as Figure 4 but for the jets emission lines in the 2017 observations. The spectrum, differential visibility phase and differential visibility amplitudes for a representative baseline are shown in the **top**, **middle** and **bottom** panels, respectively. The left panels are for the Pa α lines from the receding jet (which are blended with the Br γ stationary line), whereas the right panels correspond to the Br β lines from the approaching jet (which are blended with stationary high-order Pfund lines). The red/blue components in the spectrum show the different jet knots in the observations throughout four nights. There are strong differential visibility signatures across the lines (shown in different colors for the three different nights), which allow to fit for the spatial profile of the optical jets.

jet emission lines in the K band spectrum at this epoch are the Pa α line from the receding jet and Br β line from the approaching jet (in contrast, in Paper I jet lines from Br γ , Br δ and He I 2.056 μm fell in the K band spectrum resulting from a precessional phase ≈ 0.7). Another difference relative to Paper I is that the jet lines often have at least two different components, one of them likely resulting from a previous jet knot ejection.

The three observations over four days allowed to follow the evolution of the jet components. In particular, the two observations over consecutive nights have jet components at similar redshifts that could correspond to the same jet knots that have brightened or faded over one day. Figure 5 shows the jet emission lines and corresponding differential visibility amplitudes and phases for a given baseline for illustration.

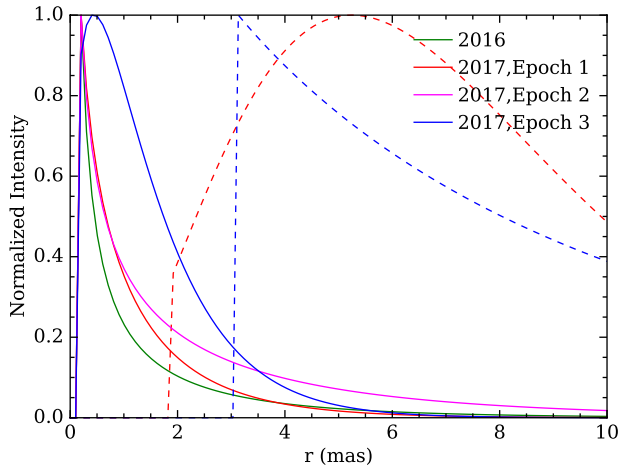


Figure 6. Collection of spatial emission profiles of the optical jets across several observations. The profiles can be divided into two classes: compact (solid lines), which peak very close to the binary and have a typical exponential profile with decay constant ~ 2 mas, and extended (dashed lines), which peak further away. The latter correspond to older jet ejections which have had more time to travel. The smooth and continuous profiles are strongly suggestive of a continuous heating mechanism along the entire jet, such as photoionization by the beamed radiation. An angular size of 1 mas corresponds to 5.5 AU for the assumed distance 5.5 kpc.

Figure 6 shows a collection of resolved spatial profiles of the optical jets over all GRAVITY observations. They can be broadly divided into two groups: compact profiles, which peak close to the accretion disk and have an exponential-like profile with decay constant ≈ 2 mas, and more extended profiles with broader shapes and which peak farther away from the binary. The latter correspond to older jet ejections which have had more time to travel along the beam.

The smooth, exponential-like spatial profiles for the optical jets suggest that the heating mechanism for the optical bullets must act smoothly along a long portion of the jet. We suggest that this is better realized through photoionization of the bullets rather than external heating processes such as interaction with a surrounding wind outflow or shocks. Although the latter had been preferred in past work (e.g. Begelman *et al.* 1980, Davidson & McCray 1980, Brown, Casinelli & Collins 1991), photoionization has also been suggested as a possible heating mechanism (Fabrika & Borisov 1987). This opens the possibility of constraining properties of the beamed radiation through spectral and spatial properties of the optical bullets.

4. Conclusion

Spectro-differential optical interferometry allows to resolve emission line structures in compact and X-ray binaries at sub-mas scale, comparable to the size of the binary orbits. GRAVITY at VLTI has significantly improved sensitivity and precision in optical interferometry, allowing observations of fainter targets at high spectral resolution with unprecedented precision in differential visibility quantities across spectral lines. We have shown two examples of X-ray binaries successfully resolved by GRAVITY. In the canonical wind-accreting BP Cru, we have resolved the inner parts of the stellar wind and found asymmetries that could probe the influence of the gravitational and radiation fields of the orbiting pulsar on the surrounding stellar environment. On the microquasar SS 433, we have found evidence for an equatorial, rotating outflow in the stationary Br γ line that carries very high specific angular momentum, and have resolved for the first time

the spatial profile of the optical jets, which is strongly suggestive of photoionization by beamed radiation as the main heating mechanism of the optical bullets.

References

- Begelman, M. C., Sarazin, C. L., Hatchett, S. P., McKee, C. F., & Arons, J. 1980, *ApJ*, 238, 722
 Blandford, R. D. & Payne, D. G., 1982, *MNRAS*, 199, 883
 Blondin, J. M. 1997, *ApJ*, 435, 756
 Blundell, K. M., Bowler, M. G., & Schmidtobreick, L. 2008, *ApJ*, 678, L47
 Blundell, K. M., Mioduszewski, A. J., Muxlow, T. W. B., Podsiadlowski, P. & Rupen, M. P., 2001, *ApJ*, 562, L79
 Borisov, N. V. & Fabrika, S. N. 1987, *Soviet Astron. Letters*, 13, 200
 Bowler, M. G. 2010, *A&A*, 521, A81
 Brown, J. C., Cassinelli, J. P., & Collins, II, G. W., 1991, *ApJ*, 378, 307
 Cechura, J. & Hadrava, P. 2015, *A&A*, 575, A5
 Cherepashchuk, A. M., Postnov, K. A., & Belinski, A. A., 2018, *MNRAS*, 479, 4844
 Davidson, K. & McCray, R., 1980, *ApJ*, 241, 1082
 Fabian, A. C. & Rees, M. J. 1979, *MNRAS*, 187, 13P
 Fabrika, S. 2004 *Space Sci. Revs*, 12, 1
 Fabrika, S. N. & Borisov, N. V., 1987, *Soviet Astron. Letters*, 13, 279
 Fabrika, S. N. & Bychkova, L. V., 1990, *A&A*, 240, L5
 Filippenko, A. V., Romani, R. W., Sargent, W. L. W., & Blandford, R. D., 1988, *AJ*, 96, 242
 Fuchs, Y., Koch Miramond, L., & Ábrahám, P. 2006, *A&A*, 445, 1041
 Gravity Collaboration, Abuter, R., Accardo, M., *et al.* 2017a, *A&A*, 602, A94
 Gravity Collaboration, Petrucci, P.-O., Waisberg, I., *et al.*, 2017b, *A&A*, 602, L11
 Hillier, D. J. & Miller, D. L. 1998, *ApJ*, 496, 407
 Illarionov, A. F. & Sunyaev, R. A. 1975, *A&A*, 39, 185
 Kaper, L., van der Meer, A. & Najarro, F. 2006, *A&A*, 457, 595
 Leahy, D. & Kostka, M. 2008, *MNRAS*, 384, 747
 Margon, B., Ford, H. C., Grandi, S. A. & Sone, R. P. S. 1979, *ApJ*, 233, L63
 Mirabel, I. F. & Rodríguez, L. F. 1994, *Nature*, 371, 46
 Paragi, Z., Vermeulen, R. C., Fejes, I., *et al.*, 1999, *A&A*, 348, 910
 Perez M., S. & Blundell, K. M. 2009, *MNRAS*, 397, 849
 Robinson, E. L., Froning, C. S., Jae, D. T. *et al.*, 2017, *ApJ*, 841, 79
 Vermeulen, R. C., Schilizzi, R. T., Spencer, R. E. *et al.* 1993, *A&A*, 270, 177
 Waisberg, I., Dexter, J., Pfuhl, O. *et al.* 2017, *ApJ*, 844, 72

Discussion

KRETSCHMAR It is fascinating to see X-ray binaries resolved at these scales. For which other sources can we expect similar results in the future?

WAISBERG The current limiting magnitude in GRAVITY for fringe tracking with the Unit Telescopes is $K \lesssim 10$ (it is possible to integrate on fainter targets if there is such a bright target within 2" but that is very rare in non-crowded fields). Unfortunately that excludes nearly all Low-Mass X-ray Binaries, but there are quite a few HMXBs besides the two presented here that are possible (e.g. some BeHMXBs). Very obscured systems that are bright in the K band but very faint in optical (such as the ones detected by INTEGRAL) should also be possible in the future once the near-infrared AO system CIAO is offered in on-axis mode.